Semiconductor Temperature Tunable Metameterial for Terahertz Applications

K. L. Koshelev[1, 2, 3] **and A. A. Bogdanov**[2, 3, 4]

[1]Saint-Petersburg State Polytechnical University, St. Petersburg 195251, Russian Federation
[2]ITMO University, St. Petersburg 197101, Russian Federation
[3]Ioffe Institute, St. Petersburg 194021, Russian Federation
[4]The Academic University, St. Petersburg 194021, Russian Federation

Abstract— We introduce a new model of homogeneous temperature tunable THz metamaterial with controllable frequency range of hyperbolic dispersion based on semiconductor superlattice with doped quantum wells. We develop a theory of quantum homogenization which is based on the Kubo formula for conductivity. The proposed approach takes into account the wave functions of the carriers, their distribution function and energy spectrum. We show that the components of the dielectric tensor of the semiconductor metamaterial can be efficiently manipulated by external temperature.

1. INTRODUCTION

Hyperbolic metamaterials (HMMs) are one of the fastest developing branches of modern optics [1–3]. The dielectric function of HMMs is described by a tensor with two different components corresponding to the directions along ($\varepsilon_\parallel$) and across ($\varepsilon_\perp$) the optical axis. Depending on the sign of these components, the crystal represents a dielectric medium ($\varepsilon_\perp > 0,\ \varepsilon_\parallel > 0$), a metal ($\varepsilon_\perp < 0,\ \varepsilon_\parallel < 0$) or a hyperbolic metamaterial ($\varepsilon_\perp \varepsilon_\parallel < 0$). For HMMs the shape of equal-frequency surface in $\mathbf{k}$-space represents a one- or two-sheet hyperboloid depending on the signature of permittivity tensor [3]. This results in a singularity of the photon density of states and explains the unique optical properties of HMMs [4].

Here we propose a new concept of an ultra homogeneous temperature tunable metamaterial based on a semiconductor superlattice for THz applications. Here, the term *ultra homogeneous* implies that the superlattice consists of coupled quantum wells separated by thin ($\sim 1\,$nm) tunnel-transparent barriers. Superlattices with barriers of such a thickness are widely used, for example, in quantum cascade lasers [5]. In this case, in contrast to a superlattice with thick barriers, quantum effects are particularly relevant and, therefore, it is incorrect to describe the dielectric function of each layer separately and then apply the homogenization procedure. Therefore, another approach, which takes into account the wave functions of the carriers, their energy spectrum modified by the superlattice potential and the carrier distribution function, should be used. We discuss the theory of proper approximation (quantum homogenization) further in Section 2.

The paper is organized as follows. In Section 2 we develop a quantum homogenization theory and derive the main equations for the effective permittivity tensor. In Sections 3 and 4, we analyze the band structure and effective dielectric function of a Te-doped GaAs/$Al_{0.3}Ga_{0.7}$As superlattice depending on the temperature and frequency of the electromagnetic field. Finally, in Section 5 we summarize our major results.

2. MODEL

2.1. Quantum Homogenization

Within the effective medium approximation, a multilayered structure with layer permittivities ε_i and layer thicknesses d_i can be considered as uniaxial optical crystal with permittivity tensor whose principle components are determined as

$$\frac{1}{\varepsilon_\parallel} = \frac{1}{d}\sum_i \frac{d_i}{\varepsilon_i}, \qquad \varepsilon_\perp = \frac{1}{d}\sum_i d_i\varepsilon_i, \qquad d = \sum_i d_i. \tag{1}$$

As we have mentioned in the introduction, these formulas are inapplicable when the thickness of the layers is comparable with electron wavelength and, therefore, quantum mechanics laws become relevant. We consider a more accurate approach based on the Kubo formula [6]. It takes into

account the distribution function of the carriers, their wave functions and spectrum modified by the superlattice potential:

$$\varepsilon_\alpha(\omega) = \varepsilon_\alpha^\infty \left(1 - \frac{\Omega_\alpha^2}{\omega(\omega + i\gamma)}\right) + \frac{4\pi i}{\omega}\sigma_\alpha(\omega). \tag{2}$$

Here and in what follows, the index $\alpha = \|, \perp$ corresponds to the directions along and across the optical axis of the metamaterial. Parameter $\varepsilon_\alpha^\infty$ is a permittivity of the lattice without free carriers, γ is inverse momentum relaxation time of the carriers which is supposed to be isotropic for simplicity.

The first term interprets classical Drude-Lorentz formula and the second term describes inter-band transitions. One can see that implementation of a superlattice in a semiconductor makes its plasma frequency anisotropic and we can distinguish plasma frequencies along ($\Omega_\|$) and across ($\Omega_\perp$) the optical axis:

$$\Omega_\alpha^2 = \frac{4\pi e^2}{\varepsilon^\infty}\frac{2}{(2\pi\hbar)^3}\sum_i \iiint f(E,\mu,T)\frac{\partial^2 E_i}{\partial p_\alpha^2}d^3p. \tag{3}$$

Here E_i is the carrier energy in the i-th miniband which depends on the momentum $\mathbf{p}$, $f(E,\mu,T)$ is the Fermi-Dirac distribution function, μ is the chemical potential, T is the temperature. The sum is over all the minibands. Here we neglect hole contribution into the plasma frequency because we will consider n-doped semiconductor structures. Eq. (3) is similar to the classical definition of plasma frequency:

$$\Omega^2 = \frac{4\pi n e^2}{\varepsilon^\infty m^*}. \tag{4}$$

Indeed, the difference between Eq. (3) and Eq. (4) is that in Eq. (3) we just average the inverse effective anisotropic mass $1/m^* = \partial^2 E/\partial p^2$ with distribution function $f(E,\mu,T)$.

In order to calculate $\Omega_\perp$ and $\Omega_\|$ we need to determine the energy spectrum $E_i(\mathbf{p})$ and the chemical potential μ.

2.2. Energy Spectrum of Carriers

Let us consider a periodic semiconductor superlattice with period d consisting of a quantum well with thickness d_1 and a barrier with thickness d_2 and height V [Fig. 1(a)]. Effective masses in the well and barrier we put equal to m_1 and m_2, respectively.

Energy dispersion of electrons in i-th miniband can be found from the dispersion equation.

$$\cos(p_\| d/\hbar) = \cos(p_1 d_1/\hbar)\cos(p_2 d_2/\hbar) - \frac{1}{2}\sin(p_1 d_1/\hbar)\sin(p_2 d_2/\hbar)\left(\frac{p_1 m_2}{p_2 m_1} + \frac{p_2 m_1}{p_1 m_2}\right) \tag{5}$$

where $p_1 = \sqrt{2m_1 E(p_\|)},\ p_2 = \sqrt{2m_2(E(p_\|) - V)}$. This dispersion equation can be obtained from the Schrödinger equation using the Floquet's theorem.

2.3. Chemical Potential

We consider the case of doped semiconductor structures on the example of a superlattice with quantum wells uniformly doped with shallow donors.

In highly doped structures, wave functions of neighbour donors can overlap. This results in a shift of donor levels and formation of a donor band. In the case of a considerable shift, the donor band can overlap with the conduction band.

The chemical potential μ can be calculated from the electroneutrality condition [7]. It states that free carrier concentration is equal to the concentration of ionized donors:

$$\sum_i \int f(\mathbf{p},\mu,T)\frac{2d^3p}{(2\pi\hbar)^3} = n_d \int \frac{g(E)dE}{2e^{(\mu-E)/(kT)} + 1} \tag{6}$$

Here n_d is the full donor concentration, $g(E)$ is a donor distribution function which can be approximated by a Gaussian with standard deviation Δ and maximum at E_d.

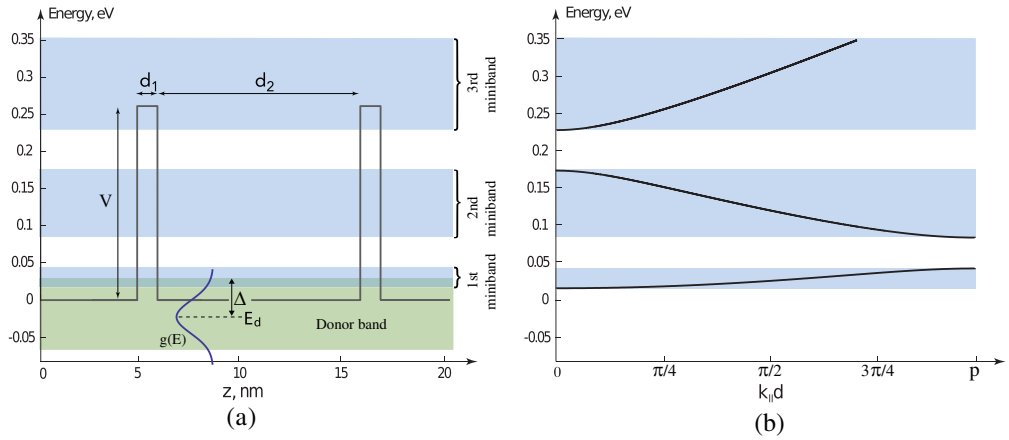

Figure 1: (a) Conduction band profile of n-doped superlattice. Blue shaded areas represent the energy of the minibands. Green shaded area corresponds to the donor band. Thicknesses of the well and the barrier are denoted as d_1 and d_2, respectively, V is the height of the barrier, $g(E)$ is a donor distribution function with standard deviation Δ and a maximum at E_d. (b) Electron energy dispersion in $GaAs/Al_{0.3}Ga_{0.7}As$ superlattice with following parameters: $d_1 = 10\,\text{mn}$, $d_2 = 1\,\text{mn}$, $V = 0.26\,\text{eV}$.

3. BAND STRUCTURE OF THE SUPERLATTICE

The model described above is applicable for superlattices of various compounds and designs. As an example, let us consider a superlattice that consists of GaAs quantum wells and $Al_{0.3}Ga_{0.7}As$ barriers. Thickness of the quantum well d_1 and the barrier d_2 we put equal to 10 and 1 nm, respectively. We consider the high frequency permittivity in Eq. (2) to be isotropic ($\varepsilon_{\parallel}^{\infty} = \varepsilon_{\perp}^{\infty}$) and put it equal to 11 [8]. The calculated band structure and electron dispersion are shown in Fig. 1(b). We consider that quantum wells are uniformly doped with Te donors with concentration $n_d = 1 \times 10^{18}\,\text{cm}^{-3}$. The energies of Te donors in bulk GaAs and in the superlattice are slightly different due to quantum confinement that arises from the superlattice potential. We neglect this difference and put $E_d = 0.03\,\text{eV}$ as in a bulk material [7]. The standard deviation of the donor distribution function Δ for such a doping level is about several hundredths of an electron-volt. In the structure under consideration we put $\Delta = 0.03\,\text{eV}$, which is in accordance with Refs. [9].

4. EFFECTIVE DIELECTRIC FUNCTION OF THE SUPERLATTICE

We calculate the frequency and temperature dependencies of the permittivity tensor components using the quantum homogenization approach [Eq. (3)]. The frequency dependence of $\varepsilon_{\perp}$ and $\varepsilon_{||}$ at room temperature is shown in Fig. 2(a). The average energy between minibands and, therefore, frequencies of interband transitions are about 0.05 eV [Fig. 1(a)], which corresponds to a frequency of 10 THz. So, the contribution of interband transition into the dielectric function [second term in Eq. (2)] can be neglected at frequencies of 1 THz without any considerable precision losses. Thus, quantum homogenization predicts that, beyond the interband transition, the tensor components of a superlattice with thin layers can be described within the classical Drude-Lorentz formula with plasma frequency described by Eq. (3).

This results qualitatively differ from effective parameters obtained within the classical homogenization procedure which predicts a resonance behaviour of $\varepsilon_{||}$ at a nonzero frequency. There is no contradiction here. Classical homogenization implies that all layers are isolated from each other and that the carriers do not move from one layer into a neighbouring one. Qualitatively it is equivalent to the restoring force that obstructs the carrier transport. This force results in an appearance of the resonance in $\varepsilon_{||}$. Quantum homogenization implies that the barriers are tunnel transparent and charges can move freely throughout the whole volume of the sample. Therefore, the dielectric function $\varepsilon_{||}$ is similar to that of a metal but takes into account interband transitions.

One can see from Fig. 2(a) that there are three frequency regions which correspond to different forms of the equal-frequency surfaces in k-space: (i) at frequencies $\omega/2\pi > 4.1\,\text{THz}$ the material behaves like a dielectric; (ii) at frequencies $2.2\,\text{THz} < \omega/2\pi < 4.1\,\text{THz}$ the form of the equal-frequency surface is a hyperboloid and the material exhibits optical properties of HMM; (iii) at $\omega/2\pi < 2.2\,\text{THz}$ electromagnetic waves decay exponentially into the medium, similar to the behaviour in a metal.

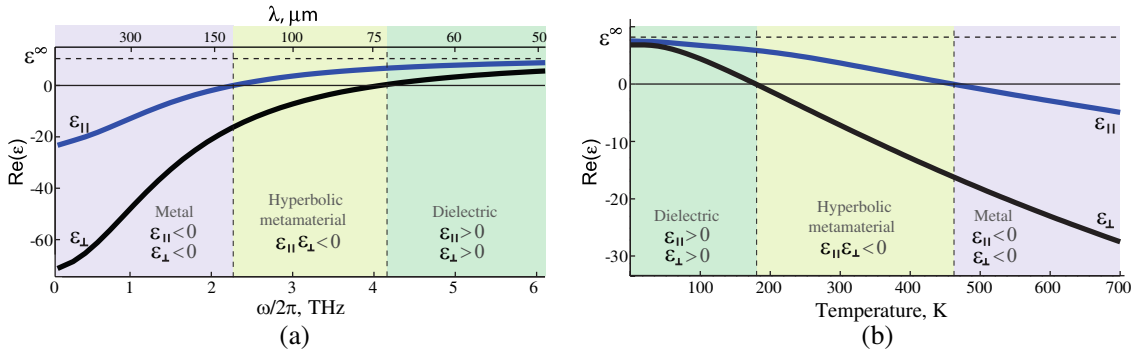

Figure 2: (a) Frequency dependence of real part of dielectric function along (blue line) and across (black line) the optical axe. Temperature $T = 300\,\mathrm{K}$. (b) Temperature dependence of real part of dielectric function along (blue line) and across (black line) the optical axis. Permittivity of the media without free carriers ε^{∞} is shown by the dashed line. Frequency $\omega/2\pi = 3\,\mathrm{THz}$.

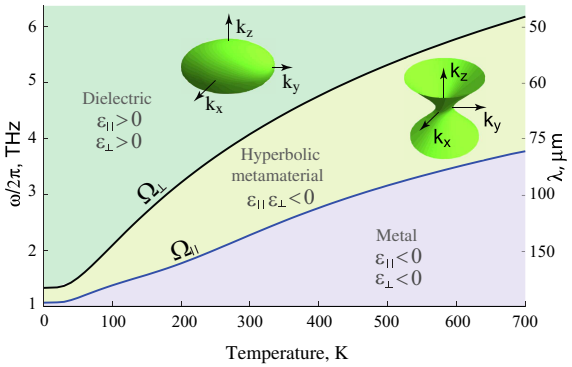

Figure 3: Temperature dependence of plasma frequency along the optical axis (blue line) and across the optical axis (black line). Insets show the shape of equal-frequency surfaces in the dielectric and hyperbolic regimes.

The temperature dependence of $\varepsilon_{\perp}$ and $\varepsilon_{||}$ at a frequency of 3 THz is shown in Fig. 2(b). One can see that the material behaves as a dielectric, HMM or a metal depending on the temperature. Dielectric dispersion can be realized at the temperature of liquid nitrogen, the hyperbolic regime is achieved at room temperature.

Figure 3 represents a topological phase state diagram. Solid lines show the temperature dependence of the longitudinal $\Omega_{||}$ and transversal $\Omega_{\perp}$ plasma frequencies. These lines divide the plane of the figure into three regions. It follows from Eq. (2) that every region corresponds to the one of the possible regimes: dielectric, metal or hyperbolic. The shapes of equal-frequency surfaces corresponding to each regimes are shown in the insets of Fig. 3.

5. CONCLUSION

In this work we proposed a new concept of an ultra homogeneous temperature-tunable metamaterial based on a doped semiconductor superlattice. We have shown that the classical homogenization procedure is inapplicable for the description of the metamaterial in terms of effective parameters because of the tunnel transparency of the barriers separating the quantum wells and that quantum homogenization should be used. We developed the theory of quantum homogenization applied to semiconductor nanostructured metamaterials. It is based on the Kubo formula for conductivity and takes into account wave functions of the carriers, their energy spectrum and distribution function.

We have shown that the components of the dielectric tensor the semiconductor metamaterial can be efficiently manipulated by external temperature. Efficient temperature tunability is a distinctive feature of semiconductors which is explained by the high sensitivity of free carrier concentration to the temperature.

A significant advantage of semiconductor metamaterials is the possibility of their direct integration into optoelectronic devices and optical integrated circuits. Moreover, semiconductor materials combine two important features. On one hand, the energy spectrum of the carriers in semiconduc-

tor nanostructures can be precisely tailored with quantum engineering technologies. On the other hand, there are many methods of dynamic control of the electron distribution function in semiconductors, which are well-developed and widely applied in nano- and optoelectronics. These are, for example, electrical injection, optical pumping, thermal excitation, electron heating by electric field, etc. The advantages mentioned earlier and the rich functionality of semiconductor metamaterials allow to consider them as important element of future optoelectronics.

ACKNOWLEDGMENT

All analytical results were obtained with a support of the Russian Foundation for Basic Research (project No. 13-02-0411) and the results of numerical simulations were obtained with a support the Russian Science Foundation (project No. 15-12-20028).

REFERENCES

1. Guo, Y., et al., "Applications of hyperbolic metamaterial substrates," *Advances Optoelectron.*, Vol. 2012, 2012.
2. Cortes, C. L., et al., "Quantum nanophotonics using hyperbolic metamaterials," *Journal of Optics*, Vol. 14, 063001, 2012.
3. Poddubny, A., et al., "Hyperbolic metamaterials," *Nature Photonics*, Vol. 7, 948–957, 2013.
4. Jacob, Z., et al., "Broadband Purcell effect: Radiative decay engineering with metamaterials," *Applied Physics Letters*, Vol. 100, 811051, 2012.
5. Gmachl, C., et al., "Recent progress in quantum cascade lasers and applications," *Reports on Progress in Physics*, Vol. 64, 1533, 2001.
6. Murayama, Y., *Mesoscopic Systems: Fundamentals and Applications*, John Wiley and Sons., 2008.
7. Sze, S. M. and K. K. Ng, *Physics of Semiconductor Devices*, John Wiley and Sons., 2006.
8. Adachi, S., *GaAs and Related Materials*, World Scientific, 1994.
9. Brody, T. P., "Nature of the valley current in tunnel diodes," *Journal of Applied Physics*, Vol. 33, 100–111, 1962.